Transactions of the Korean Society of Mechanical Engineers Vol. 6, No. 3, pp. 289~299, 1982.

<Original>

A Study on Dynamic Behavior of Connection Elements with Clearance Including Lubricating Effect

Jae Bok Yun* and Gun Bok Lee*

(Received June 14, 1982)

윤활효과를 고려한 간극이 있는 평면운동 기구의 동적거동에 관한 연구

윤 재 복·이 건 복

초 록

동적운동 기구의 연결부분에 간극이 존재함으로 인해 발생하는 충격현상을 평면운동기구를 모델로 하여 운동역학적으로 해석하였다. 비정상 상태의 Reynolds방정식을 적용하여 과도상태 및 정상 상태에 있어서 동하중과 유막 두께와의 관계를 압착 유막효과(squeeze film effect)에 중점을 두어조사 하였으며 탄성 변형을 고려하여 유도한 유막두께식과 Reynolds방정식의 수치적분으로는 무차원식으로 변형하여 Grubin의 간략해법을 이용하였다.

Nomenclature

- P : Spring force in connection elements
- α : Deformation of connection elements
- $\dot{\alpha}$: Rate of deformation
- a : Half the length of the pin
- r : Radial clearance
- D_p, D_s : Pin and sleeve diameter
- R_p, R_s : Radii of pin and sleeve
- b : Half-width of contact
- ν : Poisson's ratio
- E : Young's modulus of connection material
- M_i : Mass of i^{th} link
- J_i : Moment of inertia of i^{th} link about C.G.
- L_i : Length of the i^{th} link
- L_i^+, L_i^- : Upper and lower length of the i^{th} link
- X_i, Y_i : Linear coordinates of link center
- θ_i : Angular coordinate of the i^{th} link
- $F_{x,i}, F_{y,i}$: Joint forces in the X, Y directions on i^{th} joint
- $\vec{\delta}$: Displacement vector, represents displacement of pin center relative to sleeve center
- $\vec{v}$: Velocity vector, represents velocity of pin center relative to sleeve center
- ω_p, ω_s : Angular velocity of pin and sleeve
- ψ : Contact angle
- L : Pin length(2a)
- h : Oil filmthickness
- $\dot{h}$: Rate of change of h
- F : Total force on connection elements
- η : Material damping loss factor
- M_e : Equivalent mass
- F_{md} : Material damping force

* 正會員, 崇田大學校 機械工學科

μ : Lubricant viscosity($\mu=\mu_0 e^{\gamma p}$)
γ : Pressure viscosity constant
P : Pressure
$\vec{\tau}$: Unit vector in the direction of δ
E' : Reduced elastic modulus
$$\frac{1}{E'}=\frac{2(1-\nu^2)}{\pi E}$$
G : Material parameter ($\gamma E'$)
G_i : See equation (41)
U : Mean rolling velocity$\left(\cong\frac{1}{2}(R_s\omega_s+R_p\omega_p-\delta\dot{\theta})\right)$
R' : Relative radius of curvatuce
$$\frac{1}{R'}=\frac{1}{R_p}-\frac{1}{R_s}$$
h_0 : Minimum film thickness
H : h/R'
H_0 : h_0/R'
$\overline{P}$: Dimensionless load, $P/E'R'L$
S : $\omega R'/U$
t : Time
τ : Dimensionless time (ωt)
ω : Time base
Q : Dimensionless reduced pressure, $(1-e^{-\gamma p})/G$
ξ,ζ,χ' : Dummy variable
N : Speed parameter$\left(12\frac{\mu_0 u}{E'R'}\right)$
X : Dimensionless coordinate (x/R')

1. Introduction

Most clearances have been known to be caused by manufacturing tolerances and wear or so. They can result in the loss of performance, reduced stability, accelerated wear and initiate noise and vibration.

Clearance mechanisms show highly nonlinear dynamic behavior. In addition, inclusion of lubricant effect increases nonlinearities in terms of mathematical analysis as well as dynamic behavior. The approach to the general problem of clearances in a planar mechanism has been handled almost exclusively as kinematic approaches which provide limited information.

Lately, Dubowsky analyzed the dynamic responses due to clearances quantitatively. He introduced a simple one dimensional connection model having surface compliance, which he called "Impact Pair". He has proven to produce significant insight into the dynamic characteristics of clearance system.(12) Subsquently, he presented the result of his studies on dynamic behavior of planar mechamism with clearances. (13, 14) More recently, Rogers, R.J. modelled the pin connection using the load-deflection relationship developed by Dubowsky and included lubrication effect for the first time. (15, 16)

As for elastohydrodynamic theory, various developments account for the elastic deformation at rolling contacts simultaneously with the generation of hydrodynamic pressures in oil film. (19, 20, 21) Steady-state formulae for film thickness between two loaded surfaces have been developed by many researchers like Martin, Grubin, Dowson and Higginsson, etc. (5, 6) In the prediction of the minimum film thickness, most recently, Wang, K.L. and Cheng, H.S. calculated the minimum film thickness including almost all factors for the spur gear lubrication and Simoin, V., for Hypoid gears. (17, 18) They gave a comprehensive analysis and extensive numerical results.

This study will consider contact compliance of clearance connections and thereby determine the dynamic load and examine the lubricant film thickness variation governed by the time dependent Reynolds equations and elasticity equations. As a typical example, a slider crank mechanism is chosen and its dynamic equations will be developed by direct use of New-

ton's second law.

The followings are the objectives of the study;

1. Study of overall dynamic behavior including transient effects and prediction of film thickness in clearance joint.
2. Investigation of the influence of squeeze film effect on the minimum film thickness.

2. Basic Equations

2.1. Force-Deformation Relationship

The most common connection from an engineering point of view is the pin joint. the force-displacement relationship for an elastic pin in a circular hole was found out from a literative search. (12)

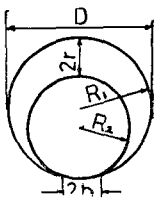

Fig.1 Connection cross section.

The force-displacement relationship is

$$\alpha=\frac{P}{2a}(K_1+K_2)\left\{\ln\frac{(R_1-R_2)8a^3e}{R_1R_2(K_1+K_2)}-\ln P\right\} \quad (1)$$

where

$$K_i=\frac{1-\nu_i^2}{\pi E_i}$$

2.2. Dynamic Equations of Planar Mechanism

The study models planar mechanism as a series of lumped masses connected by massless joints. The kinematics of the mechanism are included in the model by writing constraint equations of motion of the elements.

Fig, 2 is the link free body diagram showing the notation used to describe the dynamic parameters and the variables selected.

Applying Newton's law of motion yields;

$$F_{x,i}-F_{x,i-1}=M_i\ddot{X}_i \quad (2)$$

$$F_{y,i}-F_{y,i-1}=M_i\ddot{Y}_i \quad (3)$$

Summing Torques about the center of gravity results in

$$(F_{y,i}L_i^{+}+F_{y,i-1}L_i^{-})\cos\theta_i-(F_{x,i}L_i^{+}+F_{x,i-1}L_i^{-})\sin\theta_i+T_i-T_{i-1}+T_{ext}=J_i\ddot{\theta}_i \quad (4)$$

Constraint Equations for connection

Simple Pin Joint; Neglecting friction in the connection yields

$$T_i=0$$

In addition, the pin joint requires that the linear accelerations of the coincident points of the links should be identical. Equating the components of acceleration of common point results in;

$$\ddot{X}_i-L_i^{+}\dot{\theta}_i^2\cos\theta_i-L_i^{+}\ddot{\theta}_i\sin\theta_i=\ddot{X}_{i+1}+L_{i+1}^{-}\dot{\theta}_{i+1}^2\cos\theta_{i+1}+L_{i+1}^{-}\ddot{\theta}_{i+1}\sin\theta_{i+1} \quad (6)$$

$$\ddot{Y}_i-L_i^{+}\dot{\theta}_i^2\sin\theta_i+L_i^{+}\ddot{\theta}_i\cos\theta_i=\ddot{Y}_{i+1}+L_{i+1}^{-}\dot{\theta}_{i+1}^2\sin\theta_{i+1}-L_{i+1}^{-}\ddot{\theta}_{i+1}\cos\theta_{i+1} \quad (7)$$

Clearance Joint; The force-displacement relationship in previous paragraph relates the forces within the connection to the relative displacements along the line of contact.

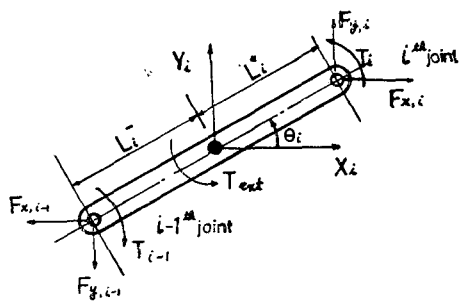

Fig. 2 i^{th} link free body diagram.

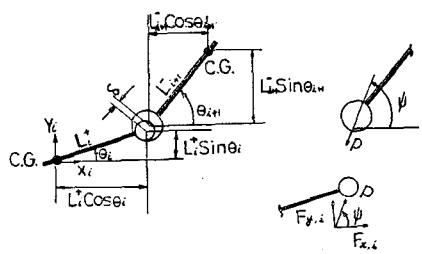

Fig. 3 Connection schematic.

The planar motion of the pin center within the bearing can be visualized the clearance circle shown in Fig. 4

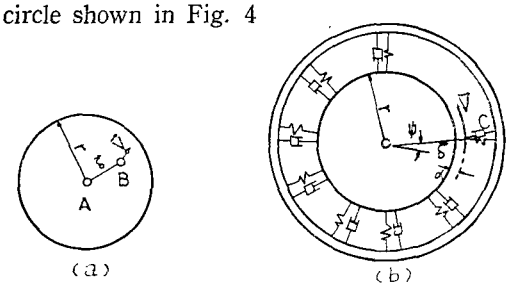

Fig.4 (a) Clearance circle. (b) Planar bearing model.

Point A represents the sleeve center and point B, pin center. $\vec{\delta}$ and $\vec{v}$ are the relative displacement and velocity of point B with respect to point A. They are expressed by the followings:

$$\vec{\delta}=\delta_x\vec{i}+\delta_y\vec{j} \tag{8}$$

$$\delta=(\delta_x{}^2+\delta_y{}^2)^{1/2} \tag{9}$$

$$\delta_x=X_{i+1}-L_{i+1}{}^-\cos\theta_{i+1}-X_i-L_i{}^+\cos\theta_i \tag{10}$$

$$\delta_y=Y_{i+1}-L_{i+1}{}^-\sin\theta_{i+1}-Y_i-L_i{}^+\sin\theta_i \tag{11}$$

$$\vec{V}=V_x\vec{i}+V_y\vec{j}=\frac{d}{dt}\delta_x\vec{i}+\frac{d}{dt}\delta_y\vec{j} \tag{12}$$

$$V_x=\dot{X}_{i+1}+L_{i+1}{}^-\dot{\theta}_{i+1}\sin\theta_{i+1}-\dot{X}_i+L_i{}^+\dot{\theta}_i\sin\theta_i \tag{13}$$

$$V_y=\dot{Y}_{i+1}-L_{i+1}{}^-\dot{\theta}_{i+1}\cos\theta_{i+1}-\dot{Y}_i-L_i{}^+\dot{\theta}_i\cos\theta_i \tag{14}$$

The contact angle is;

$$\psi=\tan^{-1}\frac{\delta_y}{\delta_x} \tag{15}$$

Thus, the force components due to contact are;

$$F_{x,i}]_s=P\cos\psi \tag{16}$$

$$F_{y,i}]_s=P\sin\psi \tag{17}$$

For the non-contact condition, the effect of the lubricant is determined by Phelan's squeeze film model which relates the bearing force F to the oil film thickness.

It is;

$$*F=-d\dot{h}/h^{1.28} \tag{18}$$

where

$$d=3.86\mu LD\left\{\left(\frac{D}{2r}\right)^2\left(\frac{L}{D}\right)^2(2r)^{0.28}\right\} \tag{19}$$

$$\dot{h}=\dot{\alpha}-|\vec{V}\cdot\vec{\tau}| \tag{20}$$

The film thickness and the rate of change of h can be obtained from combined dynamic and elastohydrodynamic equations to be developed later.

Once the spring force P is determined from connection deformation α, material damping force should be determined. The spring stiffness K is obtained by dividing P by α. Given the loss factor η and the connection equivalent mass Me, the material damping force Fmd is obtained using the following;

$$\vec{F}md=-\eta(Me\cdot k)^{1/2}\vec{v} \tag{21}$$

Then, the components of the total connection force are;

$$Fx,i=Fx,i]_s+Fx,i]md \tag{22}$$

$$Fy,i=Fy,i]_s+Fy,i]md \tag{23}$$

Remembering that the joint is assumed to be frictionless.

$$Ti=0 \tag{24}$$

Now, Equations (22) to (24) provide the required constraint relationships for the clearance connection.

2.3. Formulation of Elastohydrodynamic Equations.

Reynolds Fquation; Clearance elements operate under dynamic conditions in which the load and relative speed of rotation vary in magnitude and direction with time.

Therefore, the approach for these problems

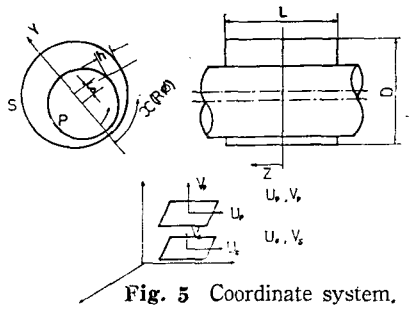

Fig. 5 Coordinate system.

* Phelan's equation will be employed with some correction.

must consider the time dependent Reynolds equation for the fluid flow.

It is;

$$\frac{\partial}{\partial x}\left(\frac{h^3}{12\mu}\frac{\partial p}{\partial x}\right)+\frac{\partial}{\partial z}\left(\frac{h^3}{12\mu}\frac{\partial p}{\partial z}\right)=\frac{\partial}{\partial x}\left(\frac{h(U_p+U_s)}{2}\right)-U_p\frac{\partial h}{\partial x}+(V_p-V_s) \tag{25}$$

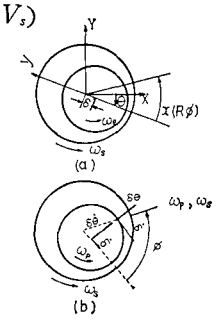

Fig. 6 Velocities.

For the system in Fig.5 and 6, the coordinate x and pertinent velocities become as follows

$$x=R_s\phi \tag{26}$$

$$U_s=R_s\omega_s \tag{27}$$

$$U_p=R_p\omega_p-\delta\sin\phi+\delta\dot{\theta}\cos\phi \tag{28}$$

$$V_p-V_s=R_p\omega_p\frac{\partial h}{\partial x}+\frac{\partial h}{\partial t} \tag{28}$$

Substituting equations (26—28) into equation (25) and neglecting lower order terms($\delta^2/R\ll1$) results in

$$\frac{1}{6}\left[\frac{\partial}{\partial x}\left(\frac{h^3}{\mu}\frac{\partial p}{\partial x}\right)+\frac{\partial}{\partial z}\left(\frac{h^3}{\mu}\frac{\partial p}{\partial z}\right)\right]=(R_s\omega_s+R_p\omega_p+\dot{\delta}\sin\phi-\delta\dot{\theta}\cos\phi)\frac{\partial h}{\partial x}+2\frac{\partial h}{\partial t} \tag{29}$$

where $\omega_s,\omega_p,\dot{\delta},\delta\dot{\theta}$ can be obtained from kinematic and dynamic relation.

At contact region, it seems reasonable to assume that $\frac{\partial p}{\partial x}$ is far higher than $\partial p/\partial z$. Or, the long bearing approximation will be made which $\partial p/\partial z$ term is neglected. Neglecting the second term reduces to

$$\frac{\partial}{\partial x}\left(\frac{h^3}{\mu}\frac{\partial p}{\partial x}\right)=6(R_s\omega_s+R_p\omega_p+\dot{\delta}\sin\phi-\delta\dot{\theta}\cos\phi)\frac{\partial h}{\partial x}+12\frac{\partial h}{\partial t} \tag{30}$$

Considering the pressure dependence of viscosity and introducing dimensionless variables, we have

$$\frac{\partial}{\partial X}\left(H^3\frac{\partial Q}{\partial X}\right)=N\left(\frac{\partial H}{\partial X}+S\frac{\partial H}{\partial \tau}\right) \tag{31}$$

The load is obtained by

$$\overline{P}=-\int\frac{\ln(1-GQ)}{G}dX \tag{32}$$

Film Thickness Formula; A film thickness $h(x)$ can be separated into three components; A constant separation induced by the lubricant film plus the rigid body separation (we use the parabolic approximation) plus the elastic distortion.

$$\text{Thus, } h=C+\frac{x^2}{2R'}+g \tag{33}$$

Where g is the combined displacement of the two bodies, represented by the following

$$g(x)=\int_{-\infty}^{\infty}P(x')\delta(x-x')dx' \tag{34}$$

$$\delta(\xi)=-\frac{2}{E'}\ln\frac{\xi}{R'}+\text{constant} \tag{35}$$

Substituting equations (34), (35) into eq. (33) and using dimensionless variables, we obtain

$$H=H_0+\frac{X^2}{2}-2\int_{-\infty}^{\infty}\overline{P}(\zeta)\ln|X-\zeta|d\zeta \tag{36}$$

Calculation of Minimum Film Thickness; The generalized theory for predictingthe transient effect in lubrication of Hertzian contact was developed by Vichard. (10) His analysis is extended and employed. Grubin assumed that for heavily loaded lubricated contacts, the existence of the film would not radically affect the pressure profile and hence the profile would be very nearly Hertzian. Under these assumptions, the film thickness can be written as the sum of uniform level Ho and Hertzian deformation He.

$$\text{or,}\quad H(x,\tau)=\text{Ho}(\tau)+\text{He}(x,\tau) \tag{37}$$

$$\text{where He}=0\text{ for }|X|\leq2\sqrt{\overline{P}} \tag{38}$$

$$He=2\overline{P}\left[-\frac{X}{2\sqrt{\overline{P}}}\sqrt{\frac{\overline{X^2}}{4\overline{P}}}-1-\ln\left(-\frac{X}{2\sqrt{\overline{P}}}+\sqrt{\frac{\overline{X^2}}{4\overline{P}}}-1\right)\right]$$

for $X<-2\sqrt{P}$ (39)

Also, Grubin assumed that the pressure is maximum when $X=0$ and at this point, Q approaches its asymptotic value $1/G$.

$$\frac{\partial Q}{\partial X}\Big]_{0,\tau}=0 \text{ and } Q(0,\tau)=1/G \quad (40)$$

After integrating eq. (31) with boundary conditions (40), substituting the relations (37)—(39) for H, we obtain

$$\frac{2\overline{P}^{3/2}}{GN}-G_p=\frac{S}{\sqrt{\overline{P}}}\left[2\frac{d\overline{P}}{d\tau}G_w-\frac{dH_0}{d\tau}\left(G_s+4\frac{\overline{P}^3}{H_0^3}\right)\right] \quad (41)$$

with

$$G_p=\int_0^1\left[z^2\sqrt{1-z^2}-z^4\ln\left(\frac{1+\sqrt{1-z^2}}{z}\right)\right]\frac{dz}{\Delta}$$

$$G_w=\int_0^1 z^3\left[\ln\left(\frac{1+\sqrt{1-z^2}}{z}\right)-\sqrt{1-z^2}\right]\frac{dz}{\Delta}$$

$$G_s=\int_0^1 z^3\frac{dz}{\Delta}$$

$$\Delta=\left[\frac{\beta z^2}{2}+\sqrt{1-z^2}-z^2\ln\left(\frac{1+\sqrt{1-z^2}}{z}\right)\right]^3$$

$\beta=H_0/\overline{P}$, z=dummy variable

The three G_i functions in eq. (41) are approximated by the following exponential functions of β

$$G_i=a_i\beta^{-bi} \quad (42)$$

where the constants a_i's and b_i's are taken from reference. (10)

3. Application to Slider Crank Mechanism

The slider crank mechanism shown in Fig. 7 is an example mechanism. The analytical approach consists of formulation of dynamic and elastohydrodynamic equations and solving these equations. The equations of motion are written by applying equations (2) through (4) to each of the four links and the three constraint relationships for each joint. In this example, the clearance connection is placed between the crank and the connection.

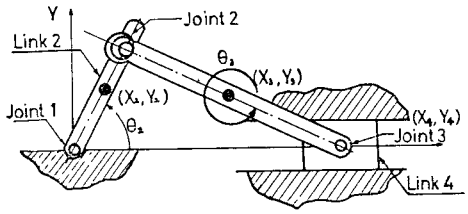

Fig. 7 Slider crank mechanism with clearance connecton.

The derived equations form completely coupled nonlinear ordinary differential equations. They must be solved simultaneously with given intial conditions. In this study, they are solved numerically using a combination of fourth order Runge-kutta and Predictor-corrector methods.

A computer program was developed to predict the variations of dynamic load as well as the lubricant film thickness. The dynamic load was assumed to be unaffected by the film thickness during contact interval but affected by equation (18) during separation.

4. Results and Discussions

4.1. Introduction

The results were obtained for a range of speeds and clearances for lubricant with isothermal exponential viscosity/pressure relationships. The scope of the results presented is limited with regard to dynamic load variation and its effect on joint film thickness. Herein, results for only two different speeds and clearances, values of practcial interest, will be presented and compared mutually because results for other ranges showed similar trends essentially. The mechanism constants are almost identical to the mechanism simulated in Ref (12), (13), as can be seen in Table 1, except that it is not off-setted. All results presented are in dimensional terms.

Table 1.

Dimension		Clearance joint cionstants
Link 1	ground	Pin diameter 0.635cm
Link 2		Pin length 1.27cm
l_2	5.08cm	$E=20,68\times10^{10}N/m^2$
M_2	0.1366kg	$\nu=0.3$
J_2	$5.37\times10^{-5}kg\cdot m^2$	Damping ratio
Link 3		$\eta=0.01$
l_3	15.24cm	viscosity (60°C)
M_3	0.3406kg	$\mu_0=0.14$ pa-sec
Slider		Pressure/viscosity constant
M_4	0.3406kg	$\gamma=1.45\times10^{-8}$ pa^{-1}

4.2. Dynamic Mechanism Behavior

Fig.8 demonstrates impact phenomena due to initial conditions in clearance joint. Results are compared with in ideal system (no clearance). As illustrated, great impact forces occur and increase significantly with the increase of forcing frequency, however, seems to be little affected by clearance size. The duration of transient regime is proportional to frquency and clearance size. High frequency content of impact pulse is seen to have the possibility of noise source. All transients decayed stably almost past the half-cycle.

Once the system comes to steady-state, connection elements remain in contact at all positions and peak force occurred at uniform position independent of frequency and clearance size, see Fig.9. (In Ref (13), which applied dry contact theory, repetitive impacts occurred with the loss of contact at two definite positions) The plots (Fig.9) represent the pin center

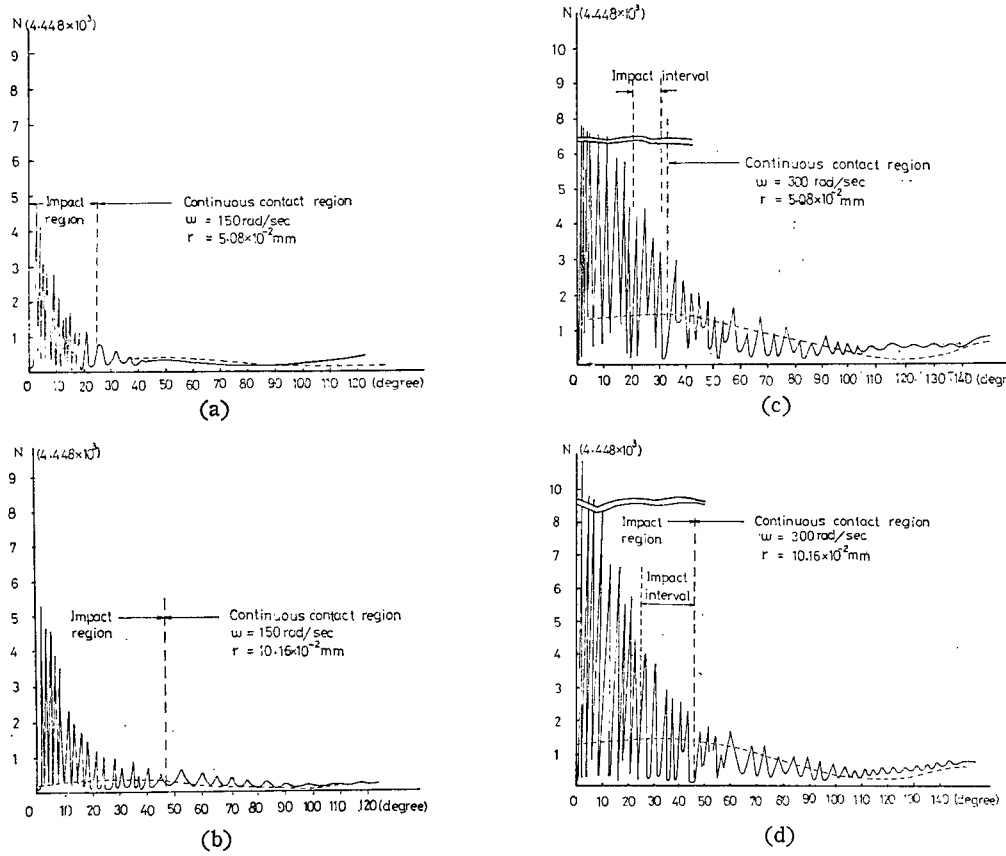

Fig. 8 Dynamic connection force in transient ragion as a function of crank angle.

paths relative to the sleeve center (circle radius equal to clearance size) in transient and steady regime. The reference frame (X, Y) is rotationally fixed in space. The diagrams show striking differences in terms of change of contact positions.

The former illustrates very arbitrary motion which repeat contact and separation very fast without any consistency, but the latter shows cyclical response which rotates at the same speed and direction at the forcing frequency. Fig.9(c) displays reverse turn occurs once in the range of 170°—180° of loading points (in ideal mechanism)

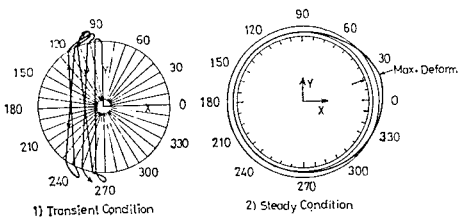

(a) Clearance; 0.0508mm (0.002 inch)
Speed ; 150 rad/sec

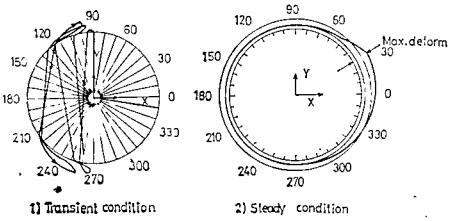

(b) Clearance; 0.1016 mm
Speed ; 150 rad/sec

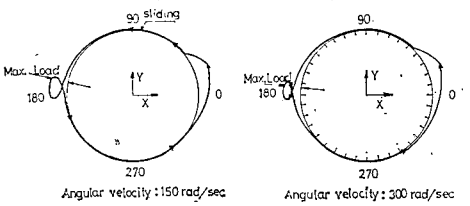

(c) Variation of loading point (no clearance)

Fig. 9 Relative motion at pin connection.

As for dynamic load in steady condition(Fig. 10), it is clear that the presence of connection clearance increases bearing forces than those in ideal system (the behavior is quite similar to that found in (13)). But this study shows that the inclusion of lubricating effect has little influence on the reduction of peak force.

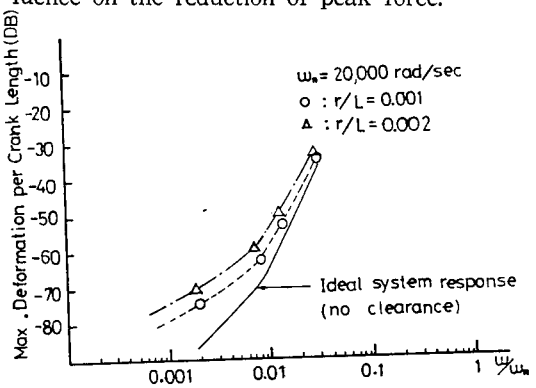

Fig. 10 Connection deformation as a function of exciting frepuency (steady-state).

4.3. Lubricating Performance

The variations of minimum film thickness in the transient zone are plotted in Fig.11

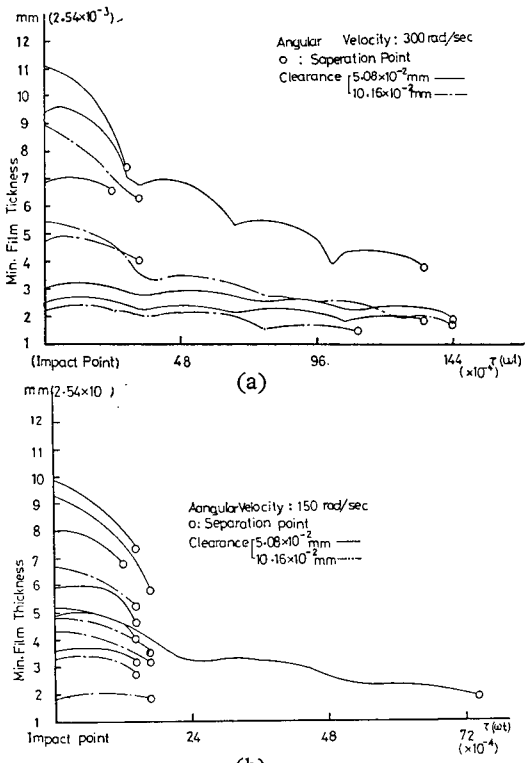

Fig. 11 Variation of dynamic film thickness (transient state).

The graphs show the variation from the instant impact occurs to separation. Film thickness varies toward a stable value somewhat rapidly or slowly depending on initial values at the impact point but reflects its slight dependence on frequency, clearance and variation of load rate.

Values are much larger over about two orders of magnitude than those according to steady theory (Ref(6), (8)). The notable feature is thought to be caused by the combined effect of elastic deformation and viscosity variation, in particular high squeeze motion. Accordingly, it is expected that such large value plays important role of the reduction of joint damage of failure while high impact load does harmful effect.

Reaching continuous contact region (Fig.12), film thickness falls to the steady-value gradually experiencing some oscillations. In steady regime(after about one cycle), the configuration shows the shape of increasing and decresing with load variation.

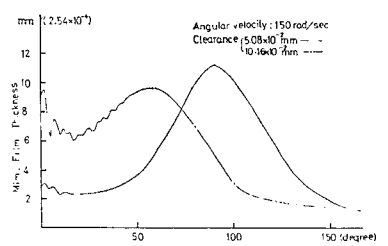

(a)

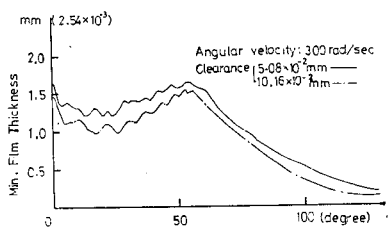

(b)

Fig. 12 Variation of dynamic film thickness (quasi steady-state).

It shows clearly that high frequency leads to highsqueeze effect. (Fig. 13)

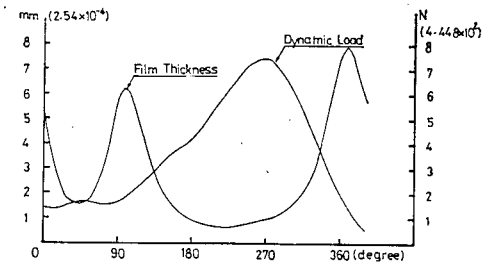

(a) Clearance 0.0508 mm, Speed 150 rad/sec.

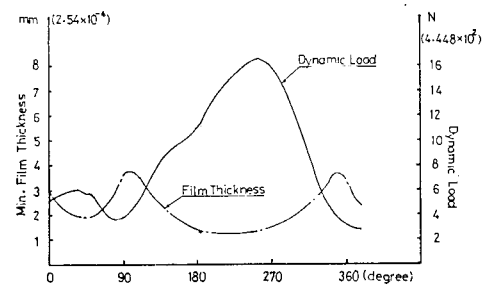

(b) Clearance 0.0508 mm, Speed 300 rad/sec.

Fig. 13 Steady-state dynamic load and film thickness as a function of crank angle.

The results are in good agreement with theoretical ones by other researchers, (6) and uphold the theory of elastohydrodynamic lubrication and squeeze effect in the analysis of these problems. However, the predicted minimum thickness of $0.17\mu m$ (6.8×10^{-6} inch) though relatively in low frequency (Fig.13(a)) is nearly equal to possible surface roughness of highest quality which is uncommon in view of engineering reality. The application of fuller theory is thought to bring about improved results.

5. Conclusions

The dynamic effects of clearance were investigated. And, also the correlation between dyn-

amic load and oil film thickness was examined by application of non-steady elasto-hydrodynamic theory. The results of simulation can draw the following conclusions.

(1) The presence of clearancecauses high dynamic load within connection regardless of the existence of lubricant. And peak force is much affected by forcing frequency, but little affected by clearance size.

(2) The duration of transient behavior increases considerably with the increase of forcing frequency and clearance.

(3) The squeeze film effect, particularly in transient state, is very outstanding with its near independence of parameter changes like frequency, clearance size and relative velocity, etc; In steady-state, more evident as the frequency increases. Therefore, we can expect that the phenomena give the favorable effect on the prevention of joint damage.

(4) The combined effects of elastic deformation and viscosity variation, squeeze motion increase the theoretical film thickness under given conditions by nearly one order of magnitude than in rigid hydrodynamic theory and gives more of engineering reality.

Acknowledgements

The authors would like to thank the SAMMI Cultural Foundation for financial support of a program of research on the title.

References

1. Landau, L.D. and Lifshitz, E.M. "Theory of Elasticity" Pergamon press Ltd.
2. Harris, T.A. "Rolling Bearing Analysis"
3. Phelan, R.M "Fundamentals of Mechanical Design" 3rd. ed., Mcgraw-Hill, New York, 1970.
4. Timoshenko, S.P. andGoodier, J.N. "Theory of Elasticity"
5. Walowit, J.A. and Anno, J.N. "Modern Developments in Lubrication Mechanics" John Wiley & sons.
6. Dowson, D. and Higginson, G.R. "Elastohydrodynamic Lubrication" Pergamon press, London 1966
7. Salbu, E.O.J. "Compressible squeeze Films and squeeze Bearings" Journal of Basic Engineering, pp. 355—366, June 1964.
8. Dowson, D. and Higginson, G.R., "A Numerical Solution to the Elastohydrodynamic problem"
9. Gupta, B.K. and Phelan, R.M., "The Load Capacity of Short Journal Bearings with oscillating Effective speed" Trans of the ASME, pp. 348—354, June 1964.
10. Vichard, J.P. "Transient Effects in the Lubrication of Hertzian Contacts" Journal of Mech. Engineering Sci. Vol. 13, No.3, pp. 173—189, 1971.
11. A. Gu., "Elastohydrodynamic Lubrication of Involute Gears" Trans of the ASME, pp. 1164—1170, November 1973.
12. Dubowsky, S. and Freudenstein, F. "Dynamic Analysis of Mechanical Systems with clearances partl, 2"
13. Dubowsky, S. "On predicting the Dynamic Effects of Clearances in planar Mechanisms"
14. Dubowsky, S. and Gardner, T.N. "Dynamic Interactions of Link Elasticity and clearance connections in planar Mechanical Systems." Trans ASME, pp. 625—661, Series B, 1975
15. Rogers, R.J. and Andrews, G.C "Dynamic Simulation of Planar Mechanical Systems with Lubricated Bearing clearances using Vector-Network Methods" Trans ASME, pp. 131—137, Febuary 1977.
16. Andrews, G.C. and Kesavan, H.K "The

Vector-Network Model: A New Approach to vector Dynamics" Mechanism and Machine Theory, pp. 57—75, Vol.10, 1975.

17. Wang, K.L. and Cheng, H.S. "A Numerica l Solution to the Dynamic Load, Film Thickness, and Surface Temperatures in Spur Gears, part 1, 2" Trans ASME, Vol. 103, pp. 177—194, 1981.
18. Simon, V. "Elastohydrodynamic Lubrication of Hypoid Gears." Trans ASME, Vol. 103, pp. 195—203, Jan 1981.
19. Childs, D and Moes, H. "Journal Bearing Impedance Descriptions for Rotordynamic Applications 1" Trans ASME, pp198—214, April 1977.
20. Evans, H.P. and Snidle, R.W. "The Isothermal Elastohydrodynamic Lubrication of Spheres" ASME journal of Lubrication Technology, Vol.103, pp. 547—557, Oct 1981.
21. Evans, H.P. and Snidle, R.W. "Inverse Solution of Reynold's Equation of Lubrication under Point-Contact Elastohydrodynamic Conditions" ASME Journal of Lubrication Technology, Vol.103, pp. 539—546, Oct 1981.